# Diterpenoids from the leaves of *Casearia kurzii* showing cytotoxic activities

Yue Liang [a], Qi Zhang [a], Xueyuan Yang [a], Ying Li [a], Xuke Zhang [a], Yuhao Li [b], Qing Du [c], Da-Qing Jin [b], Jianlin Cui [b], Namrita Lall [d], Muhetaer Tuerhong [e], Dongho Lee [f], Munira Abudukeremu [e], Jing Xu [a,g,*], Ling Shuai [a], Yuanqiang Guo [a,*]

[a] *State Key Laboratory of Medicinal Chemical Biology, College of Pharmacy, and Tianjin Key Laboratory of Molecular Drug Research, Nankai University, Tianjin 300350, People's Republic of China*

[b] *School of Medicine, Nankai University, Tianjin 300071, People's Republic of China*

[c] *Key Laboratory for Tibet Plateau Phytochemistry of Qinghai Province, College of Pharmacy, Qinghai Nationalities University, Xining 810007, People's Republic of China*

[d] *Department of Plant and Soil Sciences, University of Pretoria, Pretoria 0002, South Africa*

[e] *College of Chemistry and Environmental Sciences, Laboratory of Xinjiang Native Medicinal and Edible Plant Resources Chemistry, Kashgar University, Kashgar 844000, People's Republic of China*

[f] *Department of Biosystems and Biotechnology, College of Life Sciences and Biotechnology, Korea University, Seoul 02841, Republic of Korea*

[g] *State Key Laboratory for Chemistry and Molecular Engineering of Medicinal Resources, Guangxi Normal University, Guilin 541004, People's Republic of China*

*Corresponding authors. Tel/fax: +86-22-23502595; E-mail addresses: xujing611@nankai.edu.cn (J. Xu); victgyq@nankai.edu.cn (Y. Guo)

## HIGHLIGHTS

- Six new diterpenoids were isolated from *Casearia kurzii*.
- The structures were elucidated by NMR data and ECD calculations.
- The cytotoxic effects and mechanism were investigated.
- Compound **4** showed anti-tumor effects using *in vivo* zebrafish model.

## ABSTRACT

A phytochemical investigation to obtain bioactive substances as lead compounds or agents for cancer led to the obtainment of six new and two known clerodane diterpenoids from the leaves of *Casearia kurzii*. Their structures were elucidated using NMR techniques and electronic circular dichroism (ECD) calculations. The subsequent biological cytotoxicity evaluation of these isolates toward human lung cancer A549, human cervical cancer HeLa, human chronic myeloid leukemia K562, and human hepatocellular carcinoma HepG2 were carried out. The most active compound **4** with an $IC_{50}$ value of 9.7 $\mu$M against HepG2 cells was selected to examine the cytotoxic mechanism, which induced apoptosis and arrested the HepG2 cell cycle at S stage. The *in vivo* zebrafish experiments revealed that compound **4** had the property of inhibiting tumor proliferation and migration.


## GRAPHICAL ABSTRACT

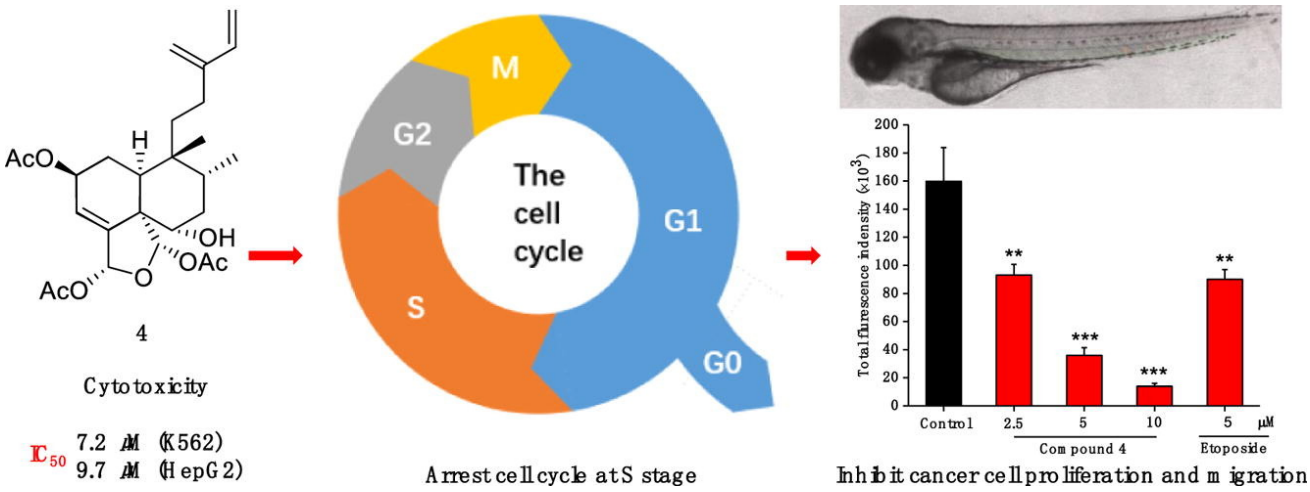



***Keywords*:** Zebrafish xenograft model; Cytotoxic activities; Apoptosis; Cell cycle; Clerodane diterpenoids; *Casearia kurzii*

## 1. Introduction

*Casearia* Jacq., a member of the Flacourtiaceae plant family, is composed of about 160 species growing widely in tropical Africa, Asia, Northwest Australia, and South America [1]. Some *Casearia* plants have been used traditionally as folk medicines to treat various diseases in different countries [2,3]. Recent phytochemical studies have revealed the presence of abundant diterpenoids, particularly clerdoane diteprenoids, in *Casearia* plants, which are a class of characteristic constituents of this genus [3-19]. These diterpenoids discovered in *Casearia* plants showed extensive biological activities [3,18,20]. The folk medicinal applications and the recent phytochemical studies of some *Casearia* plants drew our attention to the bioactive constituents in this genus.

*Casearia kurzii* C. B. Clarke. is a small tree growing in China, India, and northern Burma [2]. As a nontraditional medicinal plant, there is no record on its traditional or folk applications. In our continuous search for pharmacologically bioactive substances as potential lead compounds [21,22], the chemical constituents of *C. kurzii* were investigated. This examination led to the isolation of six new diterpenoids, named kurzipenes A–E (**1**–**6**), as well as two known analogues (**7** and **8**), from the leaves of *C. kurzii*. Their structures including absolute configurations were established on the basis of extensive NMR data analysis and comparison of electronic circular dichroism (ECD) data. All of the isolates were evaluated for their cytotoxic activities against four cancer cell lines including human hepatocellular carcinoma HepG2 cells, human lung cancer A549 cells, human chronic myeloid leukemia K562 cells, and human cervical cancer HeLa cells. Most diterpenoids showed potent cytotoxicities against these human cancer cell lines. The most active compound (**4**) was selected to investigate the cytotoxic mechanism and the *in vivo* anti-tumor effects using zebrafish model. In this paper, details of the isolation, structural determination, cytotoxic effects, preliminary action mechanism, and *in vivo* anti-tumor effects of these diterpenoids are reported here.

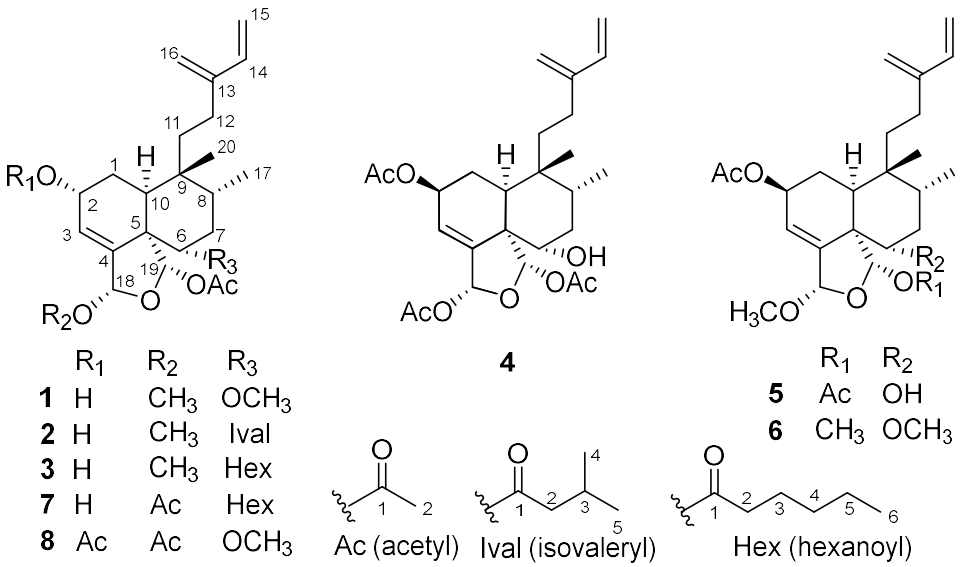


| | $R_1$ | $R_2$ | $R_3$ |
|---|---|---|---|
| **1** | H | $CH_3$ | $OCH_3$ |
| **2** | H | $CH_3$ | Ival |
| **3** | H | $CH_3$ | Hex |
| **7** | H | Ac | Hex |
| **8** | Ac | Ac | $OCH_3$ |

| | $R_1$ | $R_2$ |
|---|---|---|
| **5** | Ac | OH |
| **6** | $CH_3$ | $OCH_3$ |

**Fig. 1.** Structures of compounds **1–8.**

## 2. Experimental section

### *2.1. General experimental procedures*

The instruments for the measurement of optical rotations, IR, NMR, ECD, etc. and routine reagents for chemical isolation and biological evaluation were the same as those reported previously [23,24].

### *2.2. Plant material*

The leaves of *C. kurzii* were collected in May 2015 from Xishuangbanna, Yunnan Province, People's Republic of China. The botanical identification was made by one of the authors (Y. Guo), and a voucher specimen (No. 20150525X) was deposited at the laboratory of bioactive substance and function of natural medicines, College of Pharmacy, Nankai University.

### *2.3. Extraction and isolation*

The air-dried leaves of *C. kurzii* (14.0 Kg) were extracted with MeOH (3 × 162 L) under reflux. The organic solvent was evaporated to afford a crude methanol extract (3.1 kg), which was suspended in $H_2O$ (3.1 L) and then partitioned with petroleum ether (5 × 0.4 L) to give the petroleum ether soluble portion (540.0 g). This portion was fractionated by silica gel column chromatography (silica gel, 1200 g; column, 10 × 50 cm), using a gradient solvent system of petroleum ether-acetone (100: 0, 100: 1, 100: 2, 100: 4, 100:

6, 100: 8, 100: 11, 100: 16, 100: 22, 100: 30, 100: 40, 21 L for each gradient elution), to give 12 fractions ($F_1$–$F_{12}$) according to TLC analysis. Fraction $F_8$ was separated by MPLC over octadecylsilane (ODS) eluting with a step gradient of 63−90% MeOH in $H_2O$ to give eight subfractions $F_{8-1}$−$F_{8-8}$. The subsequent purification of $F_{8-2}$ (77% MeOH in $H_2O$) by preparative HPLC (YMC-pack ODS-AM column, 20 × 250 mm) afforded compound **1** ($t_R$ = 30 min, 8.8 mg). Compounds **2** ($t_R$ = 48 min, 9.8 mg) and **3** ($t_R$ = 40 min, 15.2 mg) were isolated from $F_{8-5}$ (83% MeOH in $H_2O$), and the fractionation of $F_{8-6}$ (80% MeOH in $H_2O$) and $F_{8-3}$ (80% MeOH in $H_2O$) led to the obtainment of compounds **4** ($t_R$ = 27 min, 7.3 mg) and **5** ($t_R$ = 32 min, 5.9 mg), respectively. Fractions $F_5$ and $F_4$, with the same procedure as for fraction $F_8$, gave subfractions $F_{5-1}$–$F_{5-7}$ and $F_{4-1}$–$F_{4-9}$, respectively. Using the same HPLC system for purification, compound **6** ($t_R$ = 39 min, 5.5 mg) was obtained from $F_{5-2}$ (85% MeOH in $H_2O$), and the purification of subfraction $F_{4-5}$ (90% MeOH in $H_2O$) resulted in the obtainment of compound **7** ($t_R$ = 32 min, 21.8 mg). Using the above MPLC, fraction $F_7$ (67–92% MeOH in $H_2O$) provided nine subfractions $F_{7-1}$–$F_{7-9}$. With the same HPLC system, compound **8** ($t_R$ = 32 min, 16.9 mg) was isolated from $F_{7-4}$ (80% MeOH in $H_2O$).

***2.3.1. Kurzipene A (1)***

Colorless oil; $[\alpha]_D^{24}$ –37.5 (*c* 0.3, $CH_2Cl_2$); ECD ($CH_3CN$) 203 ($\Delta\varepsilon$ +2.68), 225 ($\Delta\varepsilon$ –2.04) nm; IR (KBr) $\nu_{max}$ 3436, 2924, 1743, 1460, 1374, 1264, 1070, 1055, 948, 733 $cm^{-1}$; $^1H$ NMR (400 MHz, $CDCl_3$) and $^{13}C$ NMR (100 MHz, $CDCl_3$) data, see Tables 1 and 2; ESIMS *m/z* 443 $[M + Na]^+$; HRESIMS *m/z* 443.2410 $[M + Na]^+$, calcd for $C_{24}H_{36}NaO_6$, 443.2410.

**Table 1**
**$^{13}$C NMR Data for Compounds 1–6** ($\delta$ in ppm, 100 MHz, in $CDCl_3$)[a].

| Position | | 1 | | **2** | | **3** | | **4** | | **5** | | **6** | |
|---|---|---|---|---|---|---|---|---|---|---|---|---|---|
| 1 | | 30.2 | $CH_2$ | 29.4 | $CH_2$ | 29.4 | $CH_2$ | 26.3 | $CH_2$ | 26.9 | $CH_2$ | 26.6 | $CH_2$ |
| 2 | | 64.3 | CH | 63.7 | CH | 63.9 | CH | 70.8 | CH | 71.0 | CH | 71.6 | CH |
| 3 | | 126.7 | CH | 126.3 | CH | 126.2 | CH | 124.1 | CH | 126.7 | CH | 122.7 | CH |
| 4 | | 145.7 | C | 143.2 | C | 143.4 | C | 145.0 | C | 145.1 | C | 147.7 | C |
| 5 | | 51.7 | C | 52.1 | C | 52.1 | C | 53.6 | C | 51.9 | C | 54.0 | C |
| 6 | | 82.2 | CH | 74.1 | CH | 74.1 | CH | 74.2 | CH | 72.6 | CH | 83.6 | CH |
| 7 | | 32.9 | $CH_2$ | 33.2 | $CH_2$ | 33.2 | $CH_2$ | 37.5 | $CH_2$ | 35.8 | $CH_2$ | 31.7 | $CH_2$ |
| 8 | | 36.5 | CH | 36.8 | CH | 36.8 | CH | 37.6 | CH | 36.2 | CH | 36.9 | CH |
| 9 | | 37.4 | C | 37.3 | C | 37.3 | C | 38.1 | C | 38.1 | C | 38.2 | C |
| 10 | | 36.5 | CH | 36.1 | CH | 36.1 | CH | 41.0 | CH | 41.8 | CH | 40.7 | CH |
| 11 | | 27.7 | $CH_2$ | 27.9 | $CH_2$ | 27.9 | $CH_2$ | 27.6 | $CH_2$ | 27.2 | $CH_2$ | 28.2 | $CH_2$ |
| 12 | | 23.9 | $CH_2$ | 23.8 | $CH_2$ | 23.8 | $CH_2$ | 23.7 | $CH_2$ | 23.8 | $CH_2$ | 23.4 | $CH_2$ |
| 13 | | 145.4 | C | 145.4 | C | 145.4 | C | 144.4 | C | 145.0 | C | 147.3 | C |
| 14 | | 140.4 | CH | 140.3 | CH | 140.3 | CH | 140.2 | CH | 140.3 | CH | 140.1 | CH |
| 15 | | 112.5 | $CH_2$ | 112.6 | $CH_2$ | 112.7 | $CH_2$ | 112.6 | $CH_2$ | 112.6 | $CH_2$ | 112.7 | $CH_2$ |
| 16 | | 115.6 | $CH_2$ | 115.2 | $CH_2$ | 115.3 | $CH_2$ | 115.4 | $CH_2$ | 115.6 | $CH_2$ | 113.5 | $CH_2$ |
| 17 | | 15.9 | $CH_3$ | 15.6 | $CH_3$ | 15.6 | $CH_3$ | 15.7 | $CH_3$ | 15.7 | $CH_3$ | 15.9 | $CH_3$ |
| 18 | | 104.5 | CH | 103.9 | CH | 103.9 | CH | 95.1 | CH | 103.7 | CH | 103.4 | CH |
| 19 | | 98.7 | CH | 98.0 | CH | 98.0 | CH | 97.5 | CH | 98.6 | CH | 104.7 | CH |
| 20 | | 25.7 | $CH_3$ | 25.5 | $CH_3$ | 25.5 | $CH_3$ | 25.4 | $CH_3$ | 25.6 | $CH_3$ | 25.7 | $CH_3$ |
| OR-2 | 1 | | | | | | | 170.9 | C | 170.9 | C | 170.6 | C |
| | 2 | | | | | | | 21.5 | $CH_3$ | 21.3 | $CH_3$ | 21.3 | $CH_3$ |
| OR-6 | 1 | 57.9 | $CH_3$ | 172.5 | C | 173.3 | C | | | | | 57.8 | $CH_3$ |
| | 2 | | | 43.7 | $CH_2$ | 34.7 | $CH_2$ | | | | | | |
| | 3 | | | 25.5 | CH | 24.5 | $CH_2$ | | | | | | |
| | 4 | | | 22.3 | $CH_3$ | 31.3 | $CH_2$ | | | | | | |
| | 5 | | | 22.4 | $CH_3$ | 22.3 | $CH_2$ | | | | | | |
| | 6 | | | | | 13.9 | $CH_3$ | | | | | | |
| OR-18 | 1 | 56.5 | $CH_3$ | 55.5 | $CH_3$ | 55.6 | $CH_3$ | 170.0 | C | 56.2 | $CH_3$ | 55.6 | $CH_3$ |
| | 2 | | | | | | | 21.2 | $CH_3$ | | | | |
| OR-19 | 1 | 170.1 | C | 170.3 | C | 170.4 | C | 169.8 | C | 170.0 | C | 54.5 | $CH_3$ |
| | 2 | 21.8 | $CH_3$ | 21.7 | $CH_3$ | 21.8 | $CH_3$ | 21.5 | $CH_3$ | 21.7 | $CH_3$ | | |

[a] Assignments of $^1$H NMR data are based on $^1$H-$^1$H COSY, HMQC, and HMBC experiments.

**Table 2**
**$^1$H NMR data for compounds 1–6** ($\delta$ in ppm, $J$ in Hz, 400 MHz, in $CDCl_3$)[a].

| Position | 1 | 2 | 3 | 4 | 5 | 6 |
|---|---|---|---|---|---|---|
| 1$\alpha$ | 2.15 m | 2.20 m | 2.10 m | 2.11 m | 2.16 m | 2.15 m |
| 1$\beta$ | 1.93 m | 1.98 m | 1.97 m | 1.71 m | 1.73 m | 1.60 m |
| 2 | 4.41 brs | 4.40 brs | 4.41 brs | 5.60 t (8.6) | 5.56 t (8.2) | 5.52 t (8.4) |
| 3 | 6.11 d (3.2) | 6.09 d (3.6) | 6.09 d (3.8) | 5.91 s | 6.08 d (2.1) | 5.92 brs |
| 6 | 3.31 dd (11.0, 5.0) | 5.00 dd (12.9, 4.8) | 4.98 dd (12.4, 4.8) | 3.99 dd (11.9, 3.7) | 4.09 dd (11.2, 4.9) | 3.46 (11.2, 3.9) |
| 7$\alpha$ | 1.52 m | 1.67 m | 1.67 m | 1.65 m | 1.75 m | 1.45 m |
| 7$\beta$ | 1.84 m | 1.90 m | 1.90 m | 1.77 m | 1.63 m | 1.85 m |
| 8 | 1.74 m | 1.91 m | 1.91 m | 1.88 m | 1.85 m | 2.40 m |
| 10 | 2.14 dd (12.9, 4.5) | 2.35 t (8.2) | 2.32 t (8.3) | 2.35 dd (14.0, 2.0) | 2.21 dd (14.0, 2.2) | 2.39 dd (14.8, 3.0) |
| 11 | 1.43 m | 1.45 m | 1.26 m | 1.48 m | 1.45 m | 1.24 m |
| | 1.51 m | 1.52 m | 1.52 m | 1.57 m | 1.54 m | 1.52 m |
| 12 | 2.08 m | 2.10 m | 2.10 m | 2.07 m | 2.08 m | 1.96 m |
| 14 | 6.42 dd (17.6, 10.8) | 6.43 dd (17.4, 10.4) | 6.42 dd (17.6, 10.9) | 6.43 dd (17.5, 9.9) | 6.43 dd (17.6, 10.8) | 6.41 dd (17.6, 11.0) |
| 15 | 5.20 d (17.6) | 5.23 d (17.4) | 5.22 d (17.6) | 5.22 d (17.5) | 5.21 d (17.6) | 5.21 d (17.8) |
| | 5.02 d (10.8) | 5.03 d (10.4) | 5.02 d (10.9) | 5.05 d (9.9) | 5.04 d (10.8) | 5.01 d (11.0) |
| 16 | 5.03 s | 5.05 s | 5.05 s | 5.04 s | 5.05 s | 5.00 s |
| | 4.93 s | 4.94 s | 4.95 s | 4.92 s | 4.93 s | 4.96 s |
| 17 | 0.93 d (6.8) | 0.93 d (6.8) | 0.92 d (6.6) | 0.93 d (6.9) | 0.92 d (6.8) | 0.94 d (8.2) |
| 18 | 5.30 s | 5.18 s | 5.17 s | 6.71 s | 5.24 s | 5.35 s |
| 19 | 6.55 s | 6.49 s | 6.50 s | 6.42 s | 6.51 s | 4.94 s |
| 20 | 0.95 s | 0.98 s | 0.98 s | 0.95 s | 0.95 s | 0.93 s |
| OR-2 | | | | 1.90 s | 2.09 s | 2.07 s |
| OR-6 2 | 3.28 s | 2.18 m | 2.28 m | | | 3.35 s |
| 3 | | 0.90 m | 1.61 m | | | |
| 4 | | 0.88 d (6.8) | 1.30 m | | | |
| 5 | | 0.90 d (6.8) | 1.32 m | | | |
| 6 | | | 0.90 t (7.0) | | | |
| OR-18 | 3.48 s | 3.39 s | 3.40 s | 2.07 s | 3.50 s | 3.47 s |
| OR-19 | 1.85 s | 1.88 s | 1.88 s | 2.09 s | 1.85 s | 3.16 s |

[a] Assignments of $^1$H NMR data are based on $^1$H-$^1$H COSY, HMQC, and HMBC experiments.
[b] Signals were in overlapped regions of the spectra and the multiplicities could not be discerned.

### *2.3.2. Kurzipene B (2)*

Colorless oil; $[\alpha]_D^{21}$ +18.2 ($c$ 0.3, $CH_2Cl_2$); ECD ($CH_3CN$) 198 ($\Delta\varepsilon$ +8.29), 224 ($\Delta\varepsilon$ –2.00) nm; IR (KBr) $\nu_{max}$ 3448, 2926, 1730, 1462, 1373, 1222, 1164, 946, 899, 734 cm$^{-1}$; $^1$H NMR (400 MHz, $CDCl_3$) and $^{13}$C NMR (100 MHz, $CDCl_3$) data, see Tables 1 and 2; ESIMS $m/z$ 513 $[M + Na]^+$; HRESIMS $m/z$ 513.2828 $[M + Na]^+$, calcd for $C_{28}H_{42}NaO_7$, 513.2828.

### *2.3.3. Kurzipene C (3)*

Colorless oil; $[\alpha]_D^{21}$ +21.4 (*c* 0.2, $CH_2Cl_2$); ECD ($CH_3CN$) 198 ($\Delta\varepsilon$ +6.84), 220 ($\Delta\varepsilon$ –2.02) nm; IR (KBr) $\nu_{max}$ 3443, 2924, 1736, 1453, 1375, 1220, 1162, 945, 734 $cm^{-1}$; $^1H$ NMR (400 MHz, $CDCl_3$) and $^{13}C$ NMR (100 MHz, $CDCl_3$) data, see Tables 1 and 2; ESIMS *m/z* 527 $[M + Na]^+$; HRESIMS *m/z* 527.2982 $[M + Na]^+$, calcd for $C_{29}H_{44}NaO_7$, 527.2985.

### *2.3.4. Kurzipene D (4)*

Amorphous white powder; $[\alpha]_D^{21}$ −70.0 (*c* 0.2, $CH_2Cl_2$); ECD ($CH_3CN$) 196 ($\Delta\varepsilon$ –6.55), 212 ($\Delta\varepsilon$ –2.92), 220 ($\Delta\varepsilon$ –3.34) nm; IR (KBr) $\nu_{max}$ 3445, 2925, 1735, 1373, 1173, 1046, 978 $cm^{-1}$; $^1H$ NMR (400 MHz, $CDCl_3$) and $^{13}C$ NMR (100 MHz, $CDCl_3$) data, see Tables 1 and 2; ESIMS *m/z* 499 $[M + Na]^+$; HRESIMS *m/z* 499.2308 $[M + Na]^+$, calcd for $C_{26}H_{36}NaO_8$, 499.2308.

### *2.3.5. Kurzipene E (5)*

Colorless oil; $[\alpha]_D^{21}$ –97.0 (*c* 0.3, $CH_2Cl_2$); ECD ($CH_3CN$) 203 ($\Delta\varepsilon$ –5.68) nm; IR (KBr) $\nu_{max}$ 3458, 2925, 1737, 1452, 1316, 1234, 1126, 949, 894 $cm^{-1}$; $^1H$ NMR (400 MHz, $CDCl_3$) and $^{13}C$ NMR (100 MHz, $CDCl_3$) data, see Tables 1 and 2; ESIMS *m/z* 474 $[M + Na]^+$; HRESIMS *m/z* 474.2358 $[M + Na]^+$, calcd for $C_{25}H_{36}NaO_7$, 474.2359.

### *2.3.6. Kurzipene F (6)*

Colorless oil; $[\alpha]_D^{21}$ –11.7 (*c* 0.2, $CH_2Cl_2$); CD ($CH_3CN$) 198 ($\Delta\varepsilon$ –4.86) nm; IR (KBr) $\nu_{max}$ 2926, 1734, 1449, 1372, 1235, 1109, 1018, 957, 897 $cm^{-1}$; $^1H$ NMR (400 MHz, $CDCl_3$) and $^{13}C$ NMR (100 MHz, $CDCl_3$) data, see Tables 1 and 2; ESIMS *m/z* 457 $[M + Na]^+$; HRESIMS *m/z* 457.2565 $[M + Na]^+$, calcd for $C_{25}H_{38}NaO_6$, 457.2566.

### *2.4. Computational analysis*

The procedure of ECD calculations and the simulations of calculated ECD spectra were the same as described previously [24,25].

### *2.5. Cytotoxic activity assay*

The cytotoxic activities were evaluated using MTT assay [26,27]. Details on the cell culture (A549, K562, HeLa, and HepG2 cells), drug treatment were described in the Supplementary data.

### *2.6. Apoptosis analysis by flow cytometry*

The apoptosis analysis of HepG2 cells induced by the tested compound was accomplished by flow cytometry using Annexin V-FITC Apoptosis Detection Kit (Beyotime, Shanghai, People's Republic of China) according to the manufacturer's instruction [28,29]. The experimental procedure was appended in the Supplementary data.

### *2.7. Cell cycle analysis*

The distribution of cell cycle of HepG2 cells affected by the tested compound was performed using Flow cytometric analysis [30,31]. The experimental procedure was stated in the Supplementary data.

### *2.8. In vivo anti-tumor assay using zebrafish model*

Adult AB strain zebrafish were obtained from School of Medicine, Nankai University (Tianjin, People's Republic of China). Embryos were obtained from adult AB zebrafish as reported previously [32]. 48 hours post-fertilization (hpf) embryos were utilized to establish a xenograft tumor model [32,33]. In brief, K562 cells were stained with CM-Dil at a final concentration of 2.5 $\mu$g/mL. Then, the cells were suspended in FBS-free medium and adjusted to a density of $1\times10^7$ cells/mL. Subsequently, 5 nL stained cells were microinjected into the yolk sac of anesthetized zebrafish embryos and incubated for 24 h. Then, the embryos were treated with different concentrations of the selected compound by soaking and cultured at 28.5 ℃ for 48 h. At 5 days post-fertilization (dpf), K562 cells proliferation and migration in the zebrafish were examined by confocal microscopy (Leica, Germany) and ImageJ software. The density and focus number of red fluorescence represented the proliferation and migration of K562 cells *in vivo* respectively. All of the procedures involving animals were approved by the Institutional Animal Care Committee at Nankai University.

## 3. Results and discussion

### *3.1. Structural elucidation*

The petroleum ether-soluble part of the methanol extract of the leaves of *C. kurzii* was fractionated by column chromatography and purified by HPLC to afford six new and two known diterpenoids (**1**–**8**). The known diterpenoids, by comparison of the spectroscopic data with those reported in the literature, were identified as corymbulosin V (**7**) and corymbulosin M (**8**) [34].

Compound **1** was obtained as a colorless oil. Its molecular formula was determined to be $C_{24}H_{36}O_6$ through the presence of the molecular ion at *m*/*z* 443.2410 $[M + Na]^+$ (calcd for $C_{24}H_{36}NaO_6$, 443.2410) and the NMR data (Tables 1 and 2). The $^1$H NMR spectrum of **1** displayed signals for six olefinic protons [$\delta_H$ 6.11 (1H, d, $J$ = 3.2 Hz), 6.42 (1H, dd, $J$ = 17.6, 10.8 Hz), 5.20 (1H, d, $J$ = 17.6 Hz), 5.02 (1H, d, $J$ = 10.8 Hz), and 5.03 and 4.93 (each 1H, s, $H_2$-16)], and four oxygenated methine protons [$\delta_H$ 4.41 (1H, brs), 3.31 (1H, dd, $J$ = 11.0, 5.0), and 5.30 and 6.55 (each 1H, s)]. Additionally, signals for two aliphatic methyls [$\delta_H$ 0.93 (d, $J$ = 6.8 Hz) and 0.95 (3H, s)] and one acetyl methyl singlet ($\delta_H$ 1.85) were also observed from the $^1$H NMR spectrum. The $^{13}$C NMR spectrum of **1** showed 24 carbon resonances (Table 1), of which the resonances at $\delta_C$ 170.1 and 21.8, together with the methyl singlet ($\delta_H$ 1.85), indicated the presence of one acetyloxy group. In addition to this acetyloxy moiety, two methoxy groups were also deduced and defined from the carbon signals ($\delta_C$ 57.9 and 56.5) and the corresponding proton signals ($\delta_H$ 3.28 and 3.48). Apart from these carbon signals for the substituent groups, additional 20 resonances for the skeleton were displayed in the $^{13}$C NMR spectrum, including six olefinic and two acetal carbon resonances (Table 1). According to the DEPT and HMQC spectra, four olefinic carbons ($\delta_C$ 145.4, 140.4, 112.5, and 115.6) formed two sets of terminal double bonds. These NMR spectroscopic features, especially the acetal carbons ($\delta_C$ 104.5 and 98.7) and the two terminal double bonds, implied that compound **1** should be a clerodane-type diterpenoid with one acetyloxy and two methoxy groups. This skeletal type was established and confirmed as shown in Fig. 2 by 2D NMR experiments, and detailed analysis of the 1D and 2D NMR data allowed the skeletal proton and carbon signals to be attributed (Tables 1 and 2). The positions of the acetyloxy and two methoxy groups were deduced from the HMBC spectrum. The HMBC correlations of the carbon signals at $\delta_C$ 57.9 and 56.5 with the proton signals at $\delta_H$ 3.31 (H-6) and $\delta_H$ 5.30 (H-18)

demonstrated that two methoxy groups were attached at C-6 and C-18, respectively. Similarly, the acetyloxy group was found to be located at C-19 on the basis of the HMBC cross-peak of H-19 ($\delta_H$ 6.55) to carbonyl carbon signal at $\delta_C$ 170.1 of the acetyloxy group. There were no other substituent groups in **1** and one hydroxy group was assigned to C-2 based on the chemical shift of C-2 ($\delta_C$ 64.3) and the HRESIMS data. The above NMR spectroscopic analysis led to the establishment of a planar structure for **1**, which was the same as those of balanterpene G and balanterpene J [18]. However, their 1D NMR data were found to be a little different, implying compound **1** should be a stereoisomer of balanterpene G and balanterpene J. The configurational difference was further revealed by the NOESY spectrum and supported by the coupling constants.

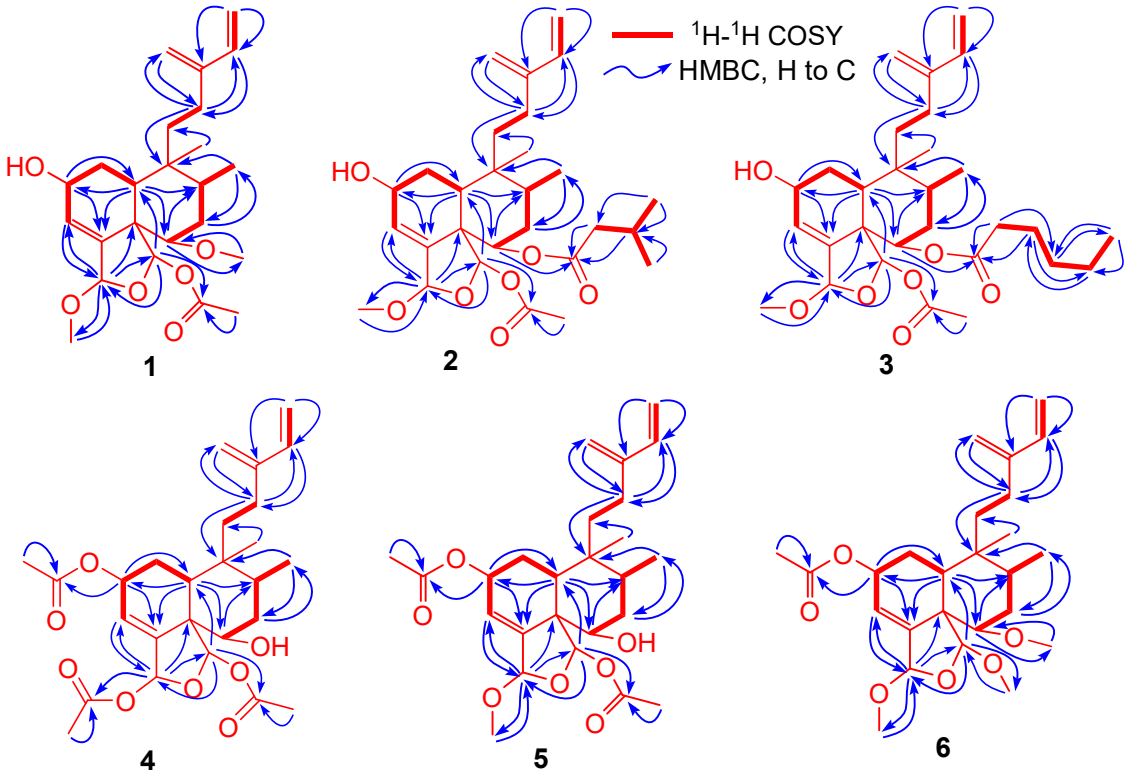


**Fig. 2.** $^1$H-$^1$H COSY and key HMBC correlations of compounds **1**–**6**.

NOESY interactions observed for H-1$\beta$/H-8, H-8/H-6, H-1$\beta$/H-6, H-18/H-19, H-19/H$_2$-11, H-7$\alpha$/H$_2$-11, H-7$\alpha$/H$_3$-17, H-10/H$_2$-11, H-1$\alpha$/H$_3$-20, together with Chem3D modeling, revealed a conformation for compound **1** as shown in Fig. 3. According to these NOE effects and the chem3D modeling, rings A and B presented a twisted chair and a normal chair conformation and were *cis*-fused with H-10 and C-19 both on the $\alpha$-side, ring C adopted an envelope conformation with H-18 and H-19 both in $\beta$-positions. Relative to

the fused rings A and B, Me-17, Me-20, the C-6 methoxy group, and the C-2 hydroxy group were assigned to be $\alpha$-, $\beta$-, $\alpha$-, and $\alpha$-oriented. The above analysis indicated that H-19 in compound **1** was a $\beta$-orientation, which differed from that of balanterpene G ($\alpha$-orientation for H-19) [18]. While, a broad singlet for H-2 and the coupling constants ($J_{2,1\alpha/\beta}$ = 0 Hz) between H-2 and $H_2$-1 also supported a $\beta$-orientation for H-2, which differed from that of balanterpene J ($\alpha$-orientation for H-2) [18]. The absolute configuration of **1** was established via comparison of the experimental and calculated ECD data, a tool to assign the absolute configuration of natural products. Through systematic conformational search and geometry optimizations by MOE and Gaussian 09, the ECD calculations at the B3LYP/SVP level with the CPCM model in acetonitrile were performed. The calculated ECD spectrum of **1** (Fig. 4A) matched the experimental data closely, which suggested an absolute configuration of 2*R*, 5*S*, 6*S*, 8*R*, 9*R*, 10*S*, 18*S*, and 19*S*. The structure of **1** was therefore elucidated as shown, and the compound was named kurzipene A.

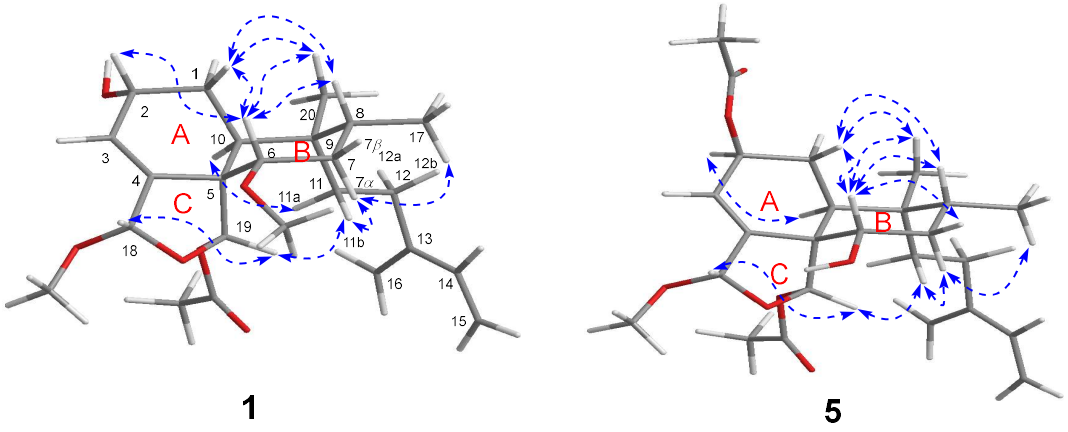


**Fig. 3.** Conformations and key NOESY correlations and of compounds **1** and **5**.

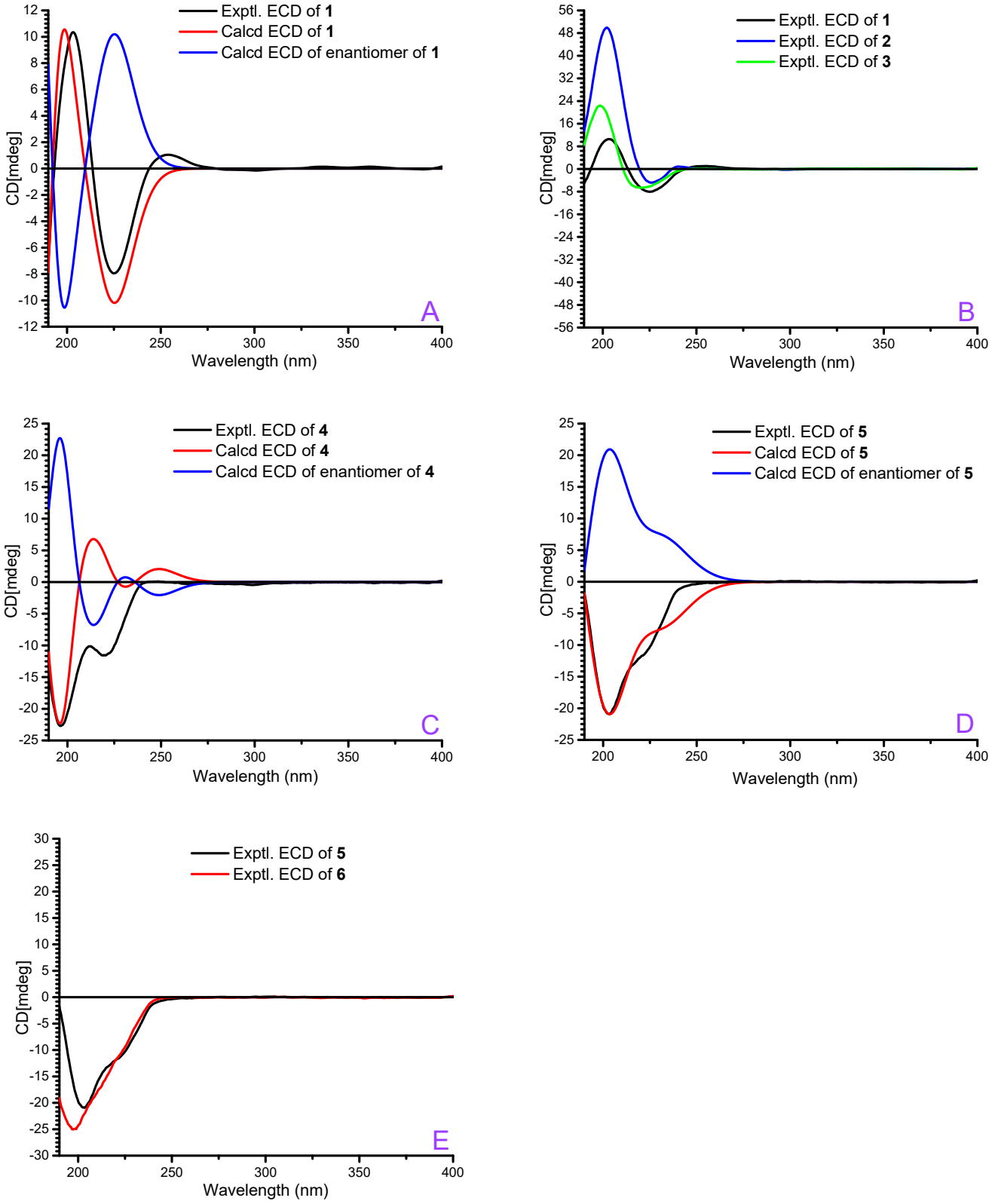


**Fig. 4.** Calculated and/or experimental ECD spectra for compounds **1**–**6** (A–E) in acetonitrile.

The molecular formula of compound **2** was determined to be $C_{28}H_{42}O_7$ based on the HRESIMS ion at *m*/*z* 513.2828 $[M + Na]^+$ (calcd for $C_{28}H_{42}NaO_7$, 513.2828) and the $^{13}C$ NMR data (Table 1). From the $^1H$ and $^{13}C$ NMR spectra, one methoxy ($\delta_{H/C}$ 3.39/55.5) and one acetoxy group ($\delta_H$ 1.88; $\delta_C$ 170.3 and 21.7)

were apparent. In addition, an isovaleryloxy moiety was deduced and defined from the observation of carbon signals ($\delta_C$ 172.5, 43.7, 25.5, 22.3, and 13.9) and the corresponding proton signals (Table 2). Apart from these carbon signals, there were 20 additional carbons for the framework in the $^{13}C$ NMR spectrum, suggesting a diterpenoid skeleton. Comparison of the chemical shifts of skeletal carbons with those of compound **1** suggested compound **2** had the same clerodane-type scaffold, as supported by the 2D NMR data. The locations of the substituent groups were determined from the HMBC correlations (Fig. 2), which disclosed the isovaleryloxy group to be located at C-6, the methoxy group at C-18, and the acetoxy groups at C-19, respectively. A hydroxy group was assigned to C-2 according to the HRESIMS data and the chemical shifts of C-2 ($\delta_C$ 63.7). The same relative configuration for compounds **1** and **2** was corroborated by detailed analysis of their NOESY spectra, where the C-2 hydroxy, C-6 isovaleryloxy, C-18 methoxy, and C-19 acetyloxy groups in compound **2** were found to be all $\alpha$-oriented. On the basis of the same relative configuration and the identical ECD spectra of compounds **1** and **2** (Fig. 4B)**,** the absolute configuration was determined as 2*R*, 5*S*, 6*S*, 8*R*, 9*R*, 10*S*, 18*S*, and 19*S*. Hence, the structure of **2** was established and named kurzipene B.

Compound **3** possessed a molecular formula $C_{29}H_{44}O_7$ based on the HRESIMS ion at *m*/*z* 527.2982 $[M + Na]^+$ (calcd for $C_{29}H_{44}NaO_7$, 527.2985). The $^{13}C$ NMR spectrum of **3** showed 29 carbon resonances, of which the signals at $\delta_C$ 170.4, 21.8, and 55.6, together with corresponding proton signals ($\delta_H$ 1.88 and 3.40), were indicative of one acetyloxy and one methoxy residue. Additionally, a hexanoyloxy group was also deduced and determined from the carbon signals ($\delta_C$ 173.3, 34.7, 24.5, 31.3, 22.3, and 13.9) and the corresponding proton signals (Table 2), which was supported by the 2D NMR data. While, the same diterpenoid skeleton of **3** as those of compounds **1** and **2** was also deduced via comparison of their $^{13}C$ NMR data (Table 1). The 2D NMR experiments evidenced the above deductions and allowed the hexanoyloxy, methoxy, and acetyloxy groups to be placed at C-6, C-18, and C-19, respectively (Fig. 2). The steric configuration of **3** was inferred from the NOESY spectrum, which was the same as those of **1** and **2**. On the basis of the same relative configuration and comparison of the ECD spectra of **1**–**3** (Fig. 4B), the absolute configuration of **3** was characterized as 2*R*, 5*S*, 6*S*, 8*R*, 9*R*, 10*S*, 18*S*, and 19*S*. Thus, the

structure of **3** was defined and named kurzipene C.

The HRESIMS of compound **4** showed a $[M + Na]^+$ ion at *m/z* 499.2308 (calcd for $C_{26}H_{36}NaO_8$, 499.2308), suggesting a molecular formula $C_{26}H_{36}O_8$ for **4**. This molecular formula was also supported by the NMR data (Tables 1 and 2). Analysis of the $^{13}C$ and $^1H$ NMR spectra of **4** (Tables 1 and 2) revealed that this compound had the same clerodane-type skeleton as compounds **1**–**3** and three acetyloxy groups. The three acetyloxy groups were found to be located at C-2, C-18, and C-19, respectively, by analysis of the HMBC spectrum, which showed long-range correlations as depicted in Fig. 2. There were no more substituent groups in compound **4** and a hydroxy group was assigned to C-6 based on the chemical shift of C-6 ($\delta_C$ 74.2) and the HRESIMS data. NOESY data analysis revealed the steric configuration of **4** was the same as those of compounds **1**–**3** except for the C-2 substituent group, which occupied a $\beta$-position differing from those of compounds **1**–**3**. The final configuration of **4** was determined by comparison of the experimental and calculated ECD data. The calculated ECD spectrum of **4** was in good agreement with the experimental data (Fig. 4C), implying an (2*S*,5*S*,6*S*,8*R*,9*R*,10*S*,18*R*,19*S*) absolute configuration. Hence, the structure of **4** was identified and named kurzipene D.

The $^1H$ and $^{13}C$ NMR spectra of compounds **5** and **6** indicated that two compounds had the same scaffold as compounds **1**–**4**. For compound **5**, besides one methoxy and two acetyloxy groups indicated by the corresponding proton and carbon signals (Tables 1 and 2), one hydroxy group should be present according to the total oxygenated carbons (Table 1) and the HRESIMS data. The methoxy and two acetyloxy groups were found to be located at C-18, C-2, and C-19 on the basis of HMBC correlations as shown in Fig. 2. Compound **6** possessed one acetyloxy and three methoxy groups according to the $^1H$ and $^{13}C$ NMR spectra (Tables 1 and 3). The acetyloxy and three methoxy groups were found to be located at C-2, C-6, C-18, and C-19, respectively, by the corresponding cross-peaks in the HMBC spectrum (Fig. 2). After determining the planar structures, the same steric configuration for compounds **5** and **6** as that of compound **4** was revealed by the careful analysis of their NOESY spectra, where the substituent groups at C-2, C-6, C-18, and C-19 were determined as $\beta$-, $\alpha$-, $\alpha$-, $\alpha$-oriented. The absolute configuration of **5** was determined as 2*S*, 5*S*, 6*S*, 8*R*, 9*R*, 10*S*, 18*S*, and 19*S* by comparison of its experimental and calculated ECD

data (Fig. 4D). Following the determination of configuration of **5**, the same relative configuration and identical experimental ECD spectra for compounds **5** and **6** (Fig. 4E) suggested a (2*S*,5*S*,6*S*,8*R*,9*R*,10*S*,18*S*,19*R*) absolute configuration for **6**. Compounds **5** and **6** were therefore characterized and named kurzipenes E and F, respectively. It should be noted that the structure of compound **6** could be found in Scifinder data base, but there has been no literature to report this structure and its NMR data.

### *3.2. Cytotoxic activities*

Cancer is a serious disease that endangers human health and has attracted extensive attention. Therefore, it is urgent to develop new drugs to treat cancer effectively. Relevant studies indicate that the discovery of bioactive natural products is of great significance to the development of new anticancer drugs [35,36]. In order to obtain bioactive natural products as lead compounds against cancer, compounds **1**–**8** obtained from the leaves of *C. kurzii* were evaluated for their cytotoxic activities against four cell lines (A549, K562, HeLa, and HepG2 cells) using MTT assay [37,38]. Etoposide was used as a positive control [39,40]. All of the compounds exhibited cytotoxic effects toward four cancer cell lines. For human hepatocellular carcinoma HepG2 cells, compounds **1**–**3**, **5**, and **6** showed weak activities with $IC_{50}$ values more than 60 $\mu$M, compound **8** exhibited moderate effects with $IC_{50}$ value of 20.6 $\mu$M, and compounds **4** and **7** showed strong cytotoxic effects with $IC_{50}$ values of 9.7 and 16.8 $\mu$M, respectively. The $IC_{50}$ values of compounds **4** and **7** cytotoxic to HepG2 cells were less than 20 $\mu$M and comparable to the positive control, etoposide ($IC_{50}$ value, 16.0 $\mu$M). For human lung cancer A549 cells, compounds **1**, **3**, **5**, and **6** were weakly effective ($IC_{50}$ values > 60 $\mu$M), compound **2** exhibited moderate effects with $IC_{50}$ value of 32.6 $\mu$M, and compounds **4**, **7**, and **8** showed promising activities with $IC_{50}$ values less than 20 $\mu$M compared to the positive control etoposide ($IC_{50}$ value, 10.4 $\mu$M). For human cervical cancer HeLa cells, compounds **4**, **7**, and **8** had strong cytotoxicities with $IC_{50}$ values of 12.4, 14.2, and 17.5 $\mu$M, respectively. Compounds **2** and **6** showed moderate effects with $IC_{50}$ values of 54.6 $\mu$M and 33.1 $\mu$M, while the other compounds were weakly cytotoxic ($IC_{50}$ values > 60 $\mu$M). For human chronic myeloid leukemia K562 cells, compounds **4,**

**7**, and **8** displayed strong cytotoxicities ($IC_{50}$ values < 20 $\mu$M), among which compounds **4** possessed promising activity with an $IC_{50}$ value of 7.2 $\mu$M. The rest compounds exhibited relatively weak cytotoxicity ($IC_{50}$ values > 60 $\mu$M). These cytotoxic data were collated in Table 3, which revealed that compound **4** was the most active toward the selected four cancer cell lines. According to the cytotoxic activity data and the structures of these compounds, compound **4** was found to be the most active, and a possible structure-activity relationship was summarized, indicating that an acetyloxy group at C-2 was necessary for cytotoxicity and an acetyloxy group at C-18 contributed to the improvement of cytotoxic activity.

**Table 3**
Cytotoxicities of compounds **1**–**8** against four human cancer cell clines.

| compound | HepG2 ($IC_{50}$, $\mu$M) | A549 ($IC_{50}$, $\mu$M) | HeLa ($IC_{50}$, $\mu$M) | K562 ($IC_{50}$, $\mu$M) |
|---|---|---|---|---|
| **1** | >60 | >60 | >60 | >60 |
| **2** | >60 | 32.6 ± 2.2 | 54.6 ± 6.4 | >60 |
| **3** | >60 | >60 | >60 | >60 |
| **4** | 9.7 ± 0.3 | 10.9 ± 0.6 | 12.4 ± 1.0 | 7.2 ± 0.4 |
| **5** | >60 | >60 | >60 | >60 |
| **6** | >60 | >60 | 33.1 ± 5.0 | >60 |
| **7** | 16.8 ± 1.0 | 11.2 ± 0.7 | 14.2 ± 1.3 | 10.3 ± 0.9 |
| **8** | 20.6 ± 2.0 | 18.4 ± 2.6 | 17.5 ± 1.6 | 16.5 ± 11.8 |
| etoposide[a] | 16.0 ± 2.4 | 10.4 ± 0.9 | 36.1 ± 5.2 | 17.9 ± 1.0 |

[a] Etoposide was used as a positive control. All results are expressed as the mean ± SD.

### *3.3. Apoptosis effects induced by compound 4*

All of the compounds were cytotoxic against four cancer cell lines and compound **4** seemed to be the most active, especially to HepG2 cells. To understand the possible cytotoxic mechanism, compound **4**, the most potent compound, was chosen to examine the apoptosis effects on HepG2 cells. HepG2 cells were treated with different concentrations (3, 9, and 27 $\mu$M) of compound **4** for 48 h, and then the cells were harvested, stained with Annexin V and propidium iodide (PI), and subsequently analyzed by flow cytometry. As presented in Fig. 5, significant apoptotic effects on HepG2 cells induced by compound **4** were observed clearly. With the increase of concentration of compound **4**, the percentage of apoptotic cells rose from 8.37% (3 $\mu$M) to 24.24% (9 $\mu$M) and 93.20% (27 $\mu$M). The data disclosed that compound **4** induced apoptosis of HepG2 cells in a dose-dependent manner.

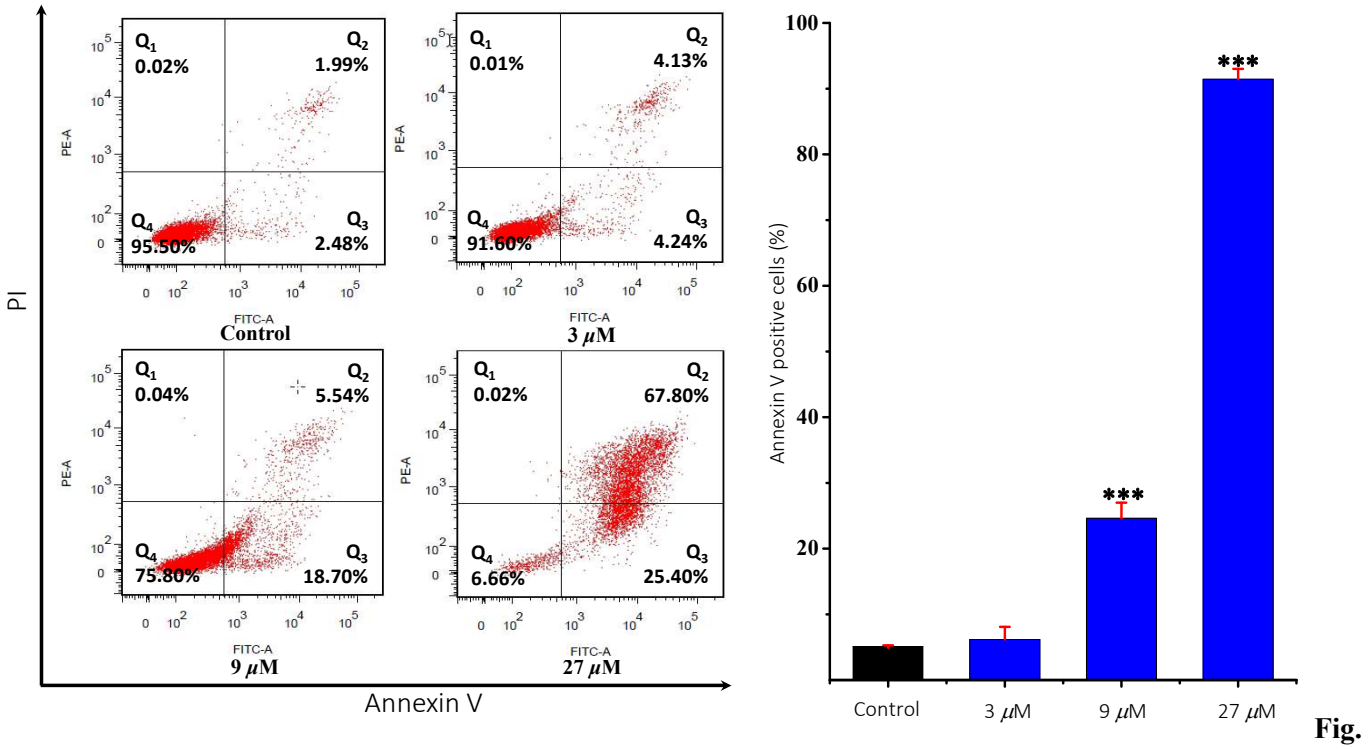


**Fig. 5.** Apoptosis effects of HepG2 induced by compound **4**. HepG2 cells were treated with different concentrations (3, 9, and 27 $\mu$M) of compound **4** for 48 h. Then the cells were harvested, stained with Annexin V and propidium iodide (PI), and subsequently analyzed by flow cytometry. Representative images (left); Representative histograms for the total numbers of cells in the early and late stages of apoptosis for the control and treatment groups data from three separate experiments expressed as means $\pm$ SD (right). (***) $p < 0.001$.

### *3.4. Effects of compound 4 on cell cycle*

Apoptosis, or programmed cell death, is closely coupled to cell cycle progression, which means interruption of cell cycle [41]. There are G1, S, G2, and M phase in cell cycle. Therefore, to better understand cytotoxic mechanism, the effects of compound **4** on the cell cycle distribution of HepG2 cells were examined, which was evaluated using flow cytometric analysis. After treated with different concentrations (6, 9, and 12 $\mu$M) of compound **4** for 48 h, the cell proportion in different phases varied following the change of concentrations. Compared to the control, the percentages of the cells in the S phase increased markedly and the cells in G1 phase decreased when treated with the concentration of 12 $\mu$M of compound **4** (Fig. 6). These data suggested that compound **4** arrested the HepG2 cell cycle at the S phage, resulting in the cell apoptosis.

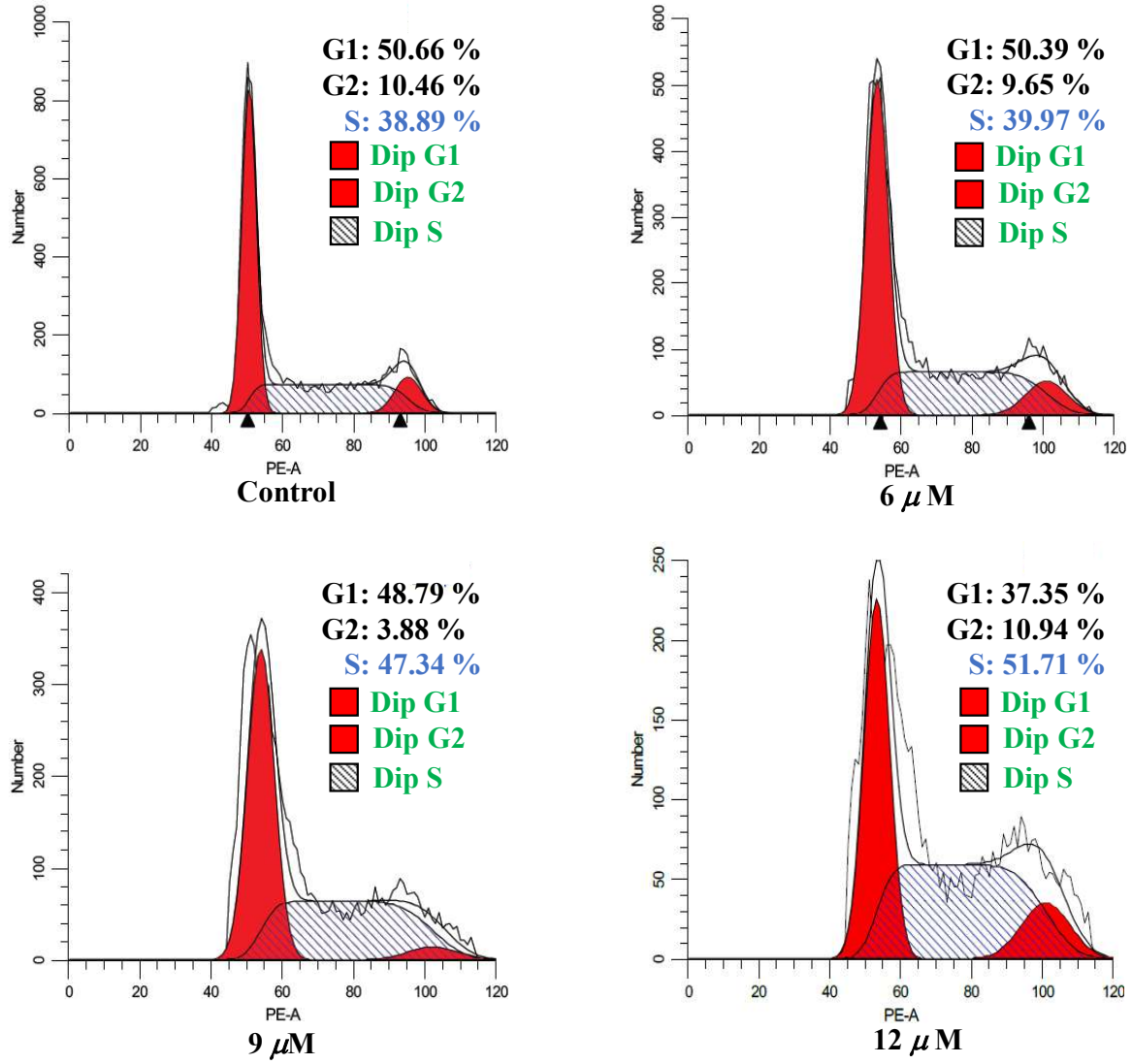


**Fig. 6.** Arrest effects of compound **4** on HepG2 cell cycle. HepG2 cells were treated with different concentrations (6, 9, and 12 $\mu$M) of compound **4** for 48 h. Then the cells were harvested and stained with propidium iodide (PI), and the cell cycle distribution was analyzed using flow cytometry.

### *3.5. In vivo anti-tumor activity of compound 4 using zebrafish model*

Xenograft tumor model is a classic way to confirm the *in vivo* effects of tested compounds on the process of tumor development *in vivo*. Zebrafish was used as an ideal animal model for its high maneuverability, short cycle, and satisfactory repeatability. Thus, to further investigate the anti-tumor effects of compound **4** *in vivo*, K562 cells were microinjected into the yolk sac of anesthetized embryos, and a xenograft tumor model using zebrafish was established [42,43]. After treatment with compound **4**, the proliferation and migration of tumor cells in zebrafish were suppressed in a dose-dependent manner. Etoposide was used as positive control. As presented in Fig. 7, compound **4** significantly decreased the intensity and foci of red fluorescence. Furthermore, compound **4** was more effective than the positive

control at the same concentration. The results showed that compound **4** effectively blocked tumor cell dissemination, invasion, and metastasis, which were comparable to the positive control, etoposide.

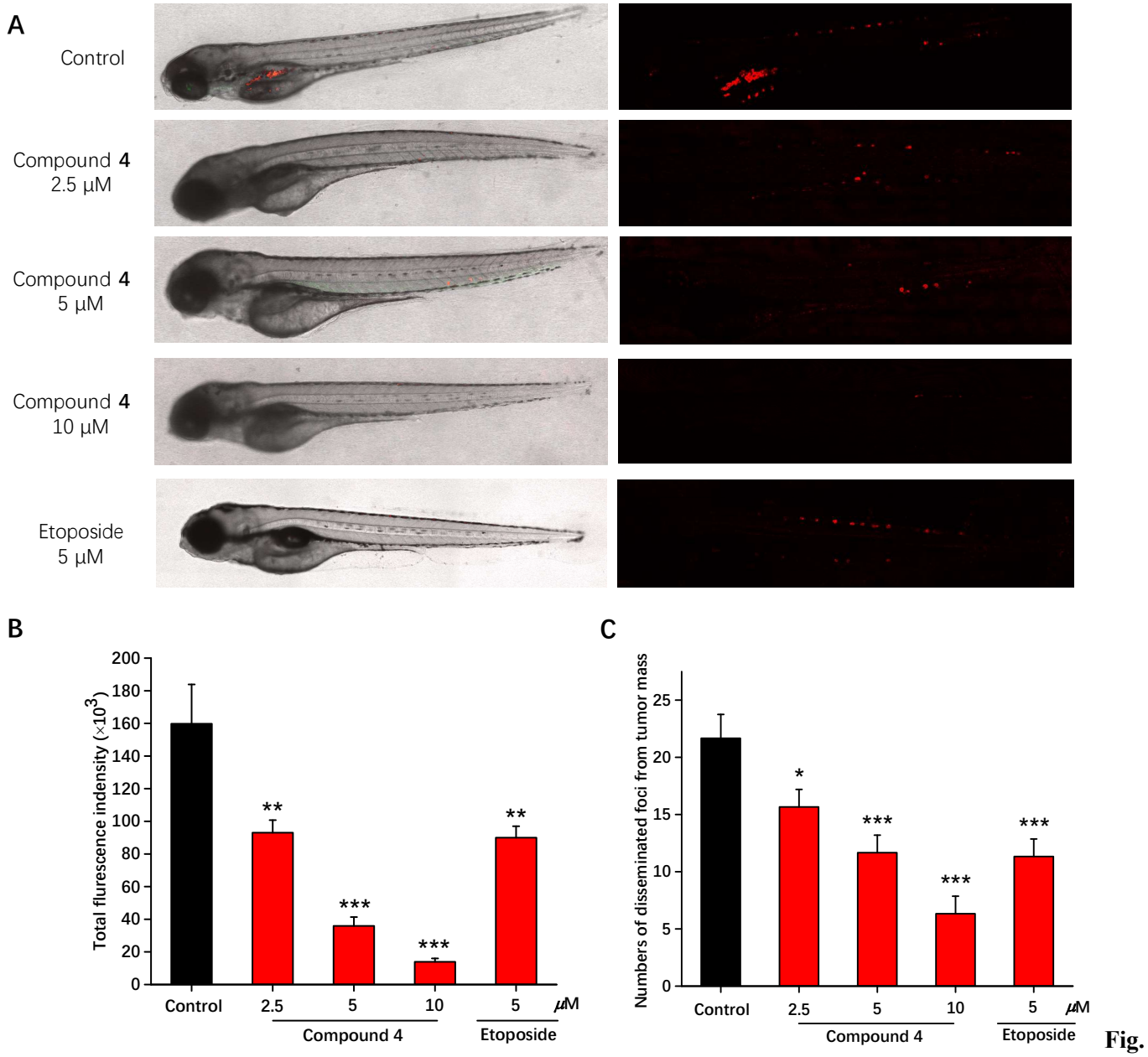


**Fig. 7.** *In vivo* anti-tumor effects of compound **4** in zebrafish xenograft. CM-DiL stained K562 cells were transplanted into 2 dpf zebrafish embryos by microinjecting. 24 h later, tumor-bearing embryos were treated with compound **4** (2.5, 5, 10 $\mu$M) and etoposide (5 $\mu$M) for 48 h. Intensity and distribution of the red fluorescence were imaged under a confocal microscope (A). Tumor proliferation (B) and metastasis (C) were quantified by ImageJ. Results were expressed as means ± SD. (*) $p < 0.5$, (**) $p < 0.01$, (***) $p < 0.001$.

## 4. Conclusion

The present phytochemical investigation on the leaves of *C. kurzii* has led to the isolation of six new clerodane diterpenoids, kurzipenes A−F (**1**−**6**) and two known diterpenoids (**7** and **8**). Their structures were elucidated on the basis of 1D and 2D NMR spectroscopic data analysis, and the absolute configurations of

**1**–**6** were established via experimental and calculated ECD data analysis. All of the compounds were evaluated for their cytotoxic activities toward A549, K562, HeLa, and HepG2 cells. Most diterpenoids showed potent cytotoxicities against the selected cancer cell lines. Compound **4** showed the most cytotoxic effects against HepG2 cells and K562 cells with $IC_{50}$ values of 9.7 $\mu$M and 7.2 $\mu$M. The preliminary mechanism investigation revealed that compound **4** induced apoptosis and arrested the HepG2 cell cycle at the S stage to exert cytotoxic effects. In addition, compound **4** showed *in vivo* anti-tumor effects by inhibiting tumor cell proliferation and migration in an *in vivo* zebrafish model.

## Conflict of interest

The authors of the present manuscript have declared that no competing interests exist.

## Acknowledgments

This research was financially supported by the National Key Research and Development Program of China (No. 2018YFA0507204), the National Natural Science Foundation of China (Nos. U1703107 and U1801288), Hundred Young Academic Leaders Program of Nankai University, the Natural Science Foundation of Tianjin (No. 19JCYBJC28100), State Key Laboratory for Chemistry and Molecular Engineering of Medicinal Resources (Guangxi Normal University, No. CMEMR2019-B01), the open project of Key Laboratory of Xinjiang Uygur Autonomous Region (Nos. 2015KL030 and 2017D04019), and the Fundamental Research Funds for the Central Universities, Nankai University (Nos. 63191142 and 63191731).

## References

[1] D. J. Newman, G. M. Cragg, J. Nat. Prod. 79 (2016) 629−661.

[2] Editorial Committee of the Flora of China, Chinese Academy of Sciences. Flora of China, Vol. 52 (1), Science Press, Beijing, 1999, pp. 69−72.

[3] L. Xia, Q. Guo, P. Tu, X. Chai, Phytochem. Rev. 14 (2015) 99−135.

[4] C. Y. Chen, Y. B. Cheng, S. Y. Chen, C. T. Chien, Y. H. Kuo, J. H. Guh, A. T. Khalil, Y. C. Shen, Chem. Biodivers. 5 (2008), 162−167.

[5] A. G. dos Santos, P. M. Ferreira, G. M. Vieira Júnior, C. C. Perez, A. Gomes Tininis, G. H. Silva, S. Bolzani Vda, L.V. Costa-Lotufo, O. Pessoa Cdo, A. J. Cavalheiro, Chem. Biodivers. 7 (2010) 205−215.

[6] P. M. Ferreira, G. C. Militao, D. J. Lima, N. D. Costa, K. C. Machado, A. G. Santos, A. J. Cavalheiro, V. S. Bolzani, D. H. Sliva, C. Pessoa, Chem. Biol. Interact. 222 (2014) 112−125.

[7] S. Kanokmedhakul, K. Kanokmedhakul, M. Buayairaksa, J. Nat. Prod. 70 (2007) 1122−1126.

[8] H. T. Nguyen, N. B. Truong, H. T. Doan, M. Litaudon, P. Retailleau, T. T. Do, H. V. Nguyen, M. V. Chau, C. V. Pham, J. Nat. Prod. 78 (2015) 2726−2730.

[9] G. M. Vieira-Júnior, L. A. Dutra, P. M. Ferreira, M. O. de Moraes, L. V. Costa Lotufo, O. Pessoa Cdo, R. B. Torres, N. Boralle, S. Bolzani Vda, A. J. Cavalheiro, J. Nat. Prod. 74 (2011) 776−781.

[10] G. M. Vieira-Júnior, T. O. Gonçalves, L. O. Regasini, P. M. Ferreira, C. O. Pessoa, L. V. Costa Lotufo, R. B. Torres, N. Boralle, V. S. Bolzani, A. J. Cavalheiro, J. Nat. Prod. 72 (2009) 1847−1850.

[11] W. Wang, J. Zhao, Y. H. Wang, T. A. Smillie, X. C. Li, I. A. Khan, Planta Med. 75 (2009) 1436−1441.

[12] W. Wang, Z. Ali, X. C. Li, I. A. Khan, Helv. Chim. Acta. 92 (2009) 1829−1839.

[13] W. Wang, Z. Ali, X. C. Li, T. A. Smillie, D. A. Guo, I. A. Khan, Fitoterapia 80 (2009) 404−407.

[14] B. Wang, X. L. Wang, S. Q. Wang, T. Shen, Y. Q. Liu, H.Q. Yuan, H. X. Lou, X. N. Wang, J. Nat. Prod. 76 (2013) 1573−1579.

[15] E. L. Whitson, C. L. Thomas, C. J. Henrich, T. J. Sayers, J. B. Mcmahon, T. C. Mckee, J. Nat. Prod. 73 (2010) 2013−2018.

[16] R. B. Williams, A. Norris, J. S. Miller, C. Birkinshaw, F. Ratovoson, R. Andriantsiferana, V. E. Rasamison, D. G. Kingston, J. Nat. Prod. 70 (2007) 206–209.

[17] J. Xu, F. Ji, X. Sun, X. Cao, S. Li, Y. Ohizumi, Y. Q. Guo, J. Nat. Prod. 78 (2015) 2648−2656.

[18] J. Xu, J. Kang, X. Sun, X. Cao, K. Rena, D. Lee, Q. Ren, S. Li, Y. Ohizumi, Y. Q. Guo, J. Nat. Prod. 79 (2016) 170−179.

[19] J. Xu, Q. Zhang, M. Wang, Q. Ren, Y. Sun, D. Q. Jin, C. F. Xie, H. Q. Chen, Y. Ohizumi, Y. Q. Guo, J. Nat. Prod. 77 (2014) 2182−2189.

[20] D. D. Bou, A. G. Tempone, E. G. Pinto, J. H. Lago, P. Sartorelli, Phytomedicine 21 (2014) 676–681.

[21] J. Ma, Q. Ren, B. Dong, Z. Shi, J. Zhang, D.Q. Jin, J. Xu, Y. Ohizumi, D. Lee, Y. Guo, Bioorg. Chem. 76 (2018) 449–457.

[22] Y. Liang, L. An, Z. Shi, X. Zhang, C. Xie, M. Tuerhong, Z. Song, Y. Ohizumi, D. Lee, L. Shuai, J. Xu, Y. Guo, J. Nat. Prod. 82 (2019) 1634–1644.

[23] J. Ma, X. Yang, Q. Zhang, X. Zhang, C. Xie, M. Tuerhong, J. Zhang, D. Q. Jin, D. Lee, J. Xu, Y. Ohizumi, Y. Q. Guo, Bioorg. Chem. 85 (2019) 558–567.

[24] F. Liu, Q. Zhang, X. Yang, Y. Xi, X. Zhang, H. Wang, J. Zhang, M. Tuerhong, D. Q. Jin, D. Lee, J. Xu, Y. Ohizumi, L. Shuai, Y. Q. Guo, Bioorg. Chem. 89 (2019) 102995.

[25] Y. Liang, L. An, Z. Shi, X. Zhang, C. Xie, M. Tuerhong, Z. Song, Y. Ohizumi, D. Lee, L. Shuai, J. Xu, Y. Guo, J. Nat. Prod. 2019, 82, 1634–1644.

[26] T. Mosmann, J. Immunol. Methods; 65 (1983) 55–63.

[27] J. Ma, Y. Cui, T. Cao, H. Xu, Y. Shi, J. Xia, Z. Wang, Cancer Lett. 460 (2019) 65−74.

[28] J. L. Tian, G. D. Yao, Y. Y. Zhang, B. Lin, Y. Zhang, L. Z. Li, X. X. Huang, S. J. Song, Bioorg. Chem. 79 (2018) 355-362.

[29] X. Hu, R. Jiao, H. Li, X. Wang, H. Lyu, X. Gao, F. Xu, Z. Li, H. Hua, D. Li, Eur. J. Med. Chem. 151 (2018) 376-388.

[30] F. Xu, X. Gao, H. Li, S. Xu, X. Li, X. Hu, Z. Li, J. Xu, H. Hua, D. Li, Bioorg. Chem. 82 (2019)192-203.

[31] W. Y. Zhao, J. J. Chen, C. X. Zou, Y. Y. Zhang, G. D. Yao, X. B. Wang, X. X. Huang, B. Lin, S. J. Song, Bioorg. Chem. 84 (2019) 309-318.

[32] A. Mazumder, H. Kang, Y. Lee, K. Kim, D. Kim, H. Shin, M. Dicato, K. Bachari, A. Silva, B. Orlikova-Boyer, M. Diederich, Cancer Lett. 438 (2018) 197−218.

[33] J. Liu, C. Huo, H. Cao, C. Fan, J. Hu, L. Deng, Z. Lu, H. Yang, L. Yu, Z. Mo, Z. Yu, Phytomedicine 61 (2019) 152843.

[34] S. Aimaiti, A. Suzuki, Y. Saito, S. Fukuyoshi, M. Goto, K. Miyake, D. J. Newman, B. R. O'Keefe, K. H. Lee, K. J. Nakagawa-Goto, J. Org. Chem. 83 (2018) 951−963.

[35] S. Gao, D. Sun, G. Wang, J. Zhang, Y. Jiang, G. Li, K. Zhang, L. Wang, J. Huang, L. Chen, Bioorg. Chem. 69 (2016) 121−128.

[36] J. S. Yu, D. Lee, S. R. Lee, J. W. Lee, C. I. Choi, T. S. Jang, K. S. Kang, K. H. Kim, Bioorg. Chem. 76 (2018) 28−36.

[37] D. H. Li, J. Y. Li, C. M. Xue, T. Han, C. M. Sai, K. B. Wang, J. C. Lu, Y. K. Jing, H. M. Hua, Z. L. Li, J. Nat. Prod. 80 (2017) 2893−2904.

[38] G. D. Yao, Q. Sun, X. Y. Song, X. X. Huang, Y. Zhang, S. J. Song, Bioorg. Chem. 77 (2018) 619−624.

[39] H. Mirzaei, M. Shokrzadeh, M. Modanloo, A. Ziar, G. H. Riazi, S. Emami, Bioorg. Chem. 75 (2017) 86−98.

[40] D. Pertuit, M. Larshini, M. A. Brahim, M. Markouk, A. C. Mitaine-Offer, T. Paululat, S. Delemasure, P. Dutartre, M. A. Lacaille-Dubois, Phytochemistry 139 (2017) 81−87.

[41] K. L. King, J. A. Cidlowski, Annu. Rev. Physiol. 60 (1998) 601−617.

[42] Y. Ye, T. Zhang, H. Yuan, D. Li, H. Lou, P. Fan, J. Med. Chem. 60 (2017) 6353−6363.

[43] C. Tseng, Y. Chen, C. Tzeng, W. Liu, C. Chou, C. Chiu, Y. Chen, Eur. J. Med. Chem. 108 (2016) 258−273.